Crytur s.r.o.
Na Lukách 2283
Turnov, 511 01
Czech Republic

26.1.2024

ESA: EISI Project Final Report

Project name:

Short-wave infrared (SWIR) high-power laser for long-distance satellite communication based on a compact laser system using Ho:YAG thin disk emitting in the 2.1 µm wavelength region

Agreement/PO number: 4000138397

Prime contractor: Crytur, spol. s r.o.

Subcontractors: HiLASE Centre, Institute of Physics of the Czech Academy of Sciences, Czech Technical University in Prague: Faculty of Nuclear Sciences and Physical Engineering – Department of Physical Electronics

Name of the authors:
Ing. Antonín Fajstavr (Crytur), Ing. Mgr. Petr Schovanec, Ph.D. (Crytur), RnDr. Jan Touš, Ph.D. (Crytur), Ing. Jiří Mužík, Ph.D. (HiLASE), Ing. Martin Smrž, Ph.D. (HiLASE), Dr. Yuya Koshiba (HiLASE), Ing. Josef Blažej, Ph.D. (CTU), Prof. Ing. Ivan Prochazka DrSc. (CTU)

Abstract:

The project of SWIR high-power thin-disk-based laser focuses on the development of the TRL 4 laser prototype for purposes of free-space laser communication. Laser communication is currently based on free space laser communication with conventional wavelengths at 1064 and 1550 nm in the infrared spectrum and still also on wavelengths in the visible spectrum. Our proposed SWIR laser prototype emits in the 2100 nm wavelength region, which introduces advanced properties of such a laser system, leading to user benefits of the laser system. The SWIR thin-disk laser project has 2 main phases: The proof of concept and the Demonstration phase. The goal of the first phase of the project was to design, construct, and demonstrate the innovative 2.1 µm laser source, the laser transmitter, in the laboratory. The system of laser receiver and laser detection were also designed and prepared. The goal of the second phase was to run the laser prototype outside the laser-dedicated laboratory and analyze beam propagation in the real environment. The high-power thin-disk laser prototype has been developed and constructed, and the performance of the laser was successfully tested in the HiLASE laboratory with the main output parameters: 6W CW laser beam, 2095 nm central wavelength, a diffraction-limited beam ($M^2 < 1.1$) in a fundamental transverse mode with near Gaussian beam quality. Beam propagation in air across short-range and mid-range distances has been simulated and analyzed. Laser beam propagation has been analyzed for 520, 640, 1064, and 1550 nm wavelengths by direct measurement. Detailed results are presented. The measured results correspond with theoretical expectations of the lower beam attenuation in the 2100 nm wavelength range in the atmosphere and the user benefits of the new proposed wavelength for free-space laser communication. The objectives of the project have been met.

Crytur s.r.o.
Na Lukách 2283
Turnov, 511 01
Czech Republic

26.1.2024

Content

Crytur s.r.o.
Na Lukách 2283
Turnov, 511 01
Czech Republic

26.1.2024

1. Introduction

Current communication with satellites at long distances or with spaceships is fundamentally based on radiofrequency communication and free space laser communication with conventional wavelengths at 1064 and 1550 nm. The project had come up with a proposal for a new regime of communication based on high-energy laser operating at Short-Wave InfraRed (SWIR) wavelengths to achieve a more stable connection and high-speed data rate, and to provide optical data link with satellites in deep space. The proposed SWIR laser solution is based on Ho:YAG (Holmium-doped Yttrium Aluminum Garnet) thin-disk material emitting laser radiation in the 2100 nm wavelength range. This new wavelength together with the thin-disk solution provides an enhanced range of use.

The goal of the ESA OSIP project has been set to build a functional prototype of the innovative Ho:YAG thin-disk laser system running continuously at a power of 5 Watts at the selected wavelength close to 2.1 µm, and to systematically evaluate its properties for atmospheric propagation under different environmental conditions within a measurement.

The main tasks of the project were defined as:

- Design of the laser sources for the 2100 nm wavelength
- Design, manufacturing, and preparation of the laser-active material
- Design of all optical components consisting of the laser source and the laser transmitter
- Construction of the laser source
- Testing and characterization of the laser source in the laser laboratory environment
- Preparation of the support lasers and equipment for experimental measurement
- Moving the laser to the location selected for experimental measurement
- Experimental measurement of the laser beams propagation

The initial status of the Technology Readiness Level (TRL) before the start of the project was 2, at the end of the project the TRL was 4, meeting the scope of the project.

2. Work package description

The project has been divided into the following fundamental steps, different work packages:

WP1 - **Design and construction of a prototype:** of the solid-state SWIR laser emitting at one or several wavelengths in the range close to 2.1 um for direct measurement of the free-space optical propagation

WP2 – **Laser transmitter and receiver optics:** Based on previous models of the atmospheric behavior and on simulations of laser beam propagation to identify proper detection systems and design suitable testing procedures

WP3 - **Testing of light propagation** under real atmospheric conditions and evaluation of benefits of the proposed idea.

In WP 1, a pump laser running at a wavelength of 1908 nm has been designed. Shaped by a proper system of collimation lenses optimizing the beam for pumping of thin disk gain medium, the pump laser was fiber-coupled to the main laser head. The pump laser was be optimized for running in a continuous-wave regime, driving a special laser head designed to pump efficiently the Ho-based thin disk. The laser head included a Ho:YAG thin-disk with a proper cooling design (in the demonstration phase water-cooled, for airborne applications it would be modified), and a system

Crytur s.r.o.
Na Lukách 2283
Turnov, 511 01
Czech Republic

26.1.2024

of optical mirrors that will form a signal beam in the optical resonator. The mirrors will be also specifically designed to cover the wavelengths in the SWIR range.

In WP 2, the CW output of the SWIR laser will be spatially expanded and collimated through proper lenses and mirrors designed especially for this application to allow long-distance, low-divergence free-space propagation. An optical system receiving the free-space laser beam, and a detection system on the receiver side will be identified and set up.

In WP 3, a set of beam propagation tests at one or several wavelengths, and an analysis of the beam by the designed detection system have been performed. The measurement was repeated under several different conditions, analyzed, and compared with the results achieved with conventional communication wavelengths.

3. WP1 - Laser source design and preparation

The HiLASE center of the IoP CAS institute has prepared the detailed layout of the laser sources. The layout was discussed and reviewed. The laser sources setup is defined in the following layout:

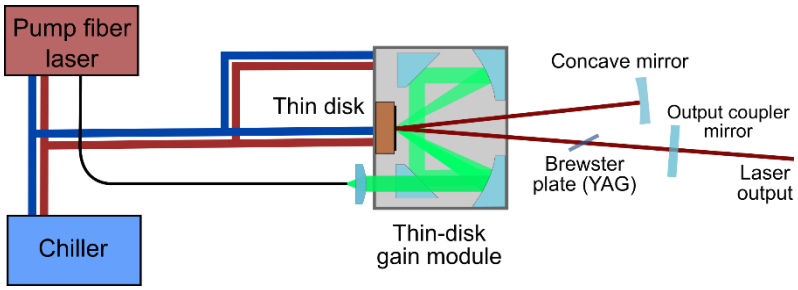

Figure 1 – source without transmitter optics

The final pump source of the 2.1 µm thin-disk laser is a thulium fiber laser with emission wavelength of 1908 nm and available power output up to 13W. The Thulium fiber laser pumps the thin-disk module (thin-disk laser head) containing the Ho:YAG thin-disk crystal. The thin-disk module is a part of the laser cavity (optical resonator), forming the 2.1 µm laser.

3.1. Laser active media – Ho:YAG thin disk

The laser active media – parameters of the Holmium thin disks defined and simulated. 6 pieces of the thin disks were fully manufactured including processes of Ho-YAG bonding, HR, and AR optical layers coating by Crytur. Figure 2 shows the resulting Ho-YAG thin-disks created for the Thin-disk laser module. The disks had 1.5 at.% Ho^{3+} concentration, their diameter was 8 mm, and were manufactured in two different versions, with thickness of 250 µm and 400 µm.

Crytur s.r.o.
Na Lukách 2283
Turnov, 511 01
Czech Republic

26.1.2024

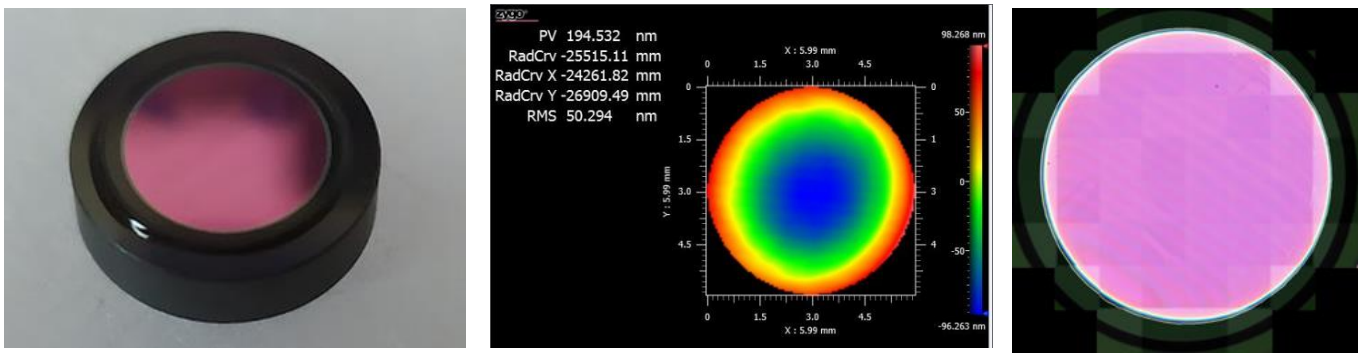

Figure 2 - Laser active media manufactured

The laser crystals were designed to be integrated into the system of laser transmitter including laser beam resonator tuning, beam expander I and II, beam attenuator, and system of laser steering. Figure 9 shows the final design layout of the system of the laser transmitter. More details of the laser transmitter are in section 5.

3.2. Fiber pump laser development

In order to obtain optical gain with the Ho:YAG thin-disk, a continuous-wave Tm:fiber operating at wavelength of 1908 nm was developed at HiLASE. The active thulium-doped fiber was pumped using fiber-coupled diode lasers with maximum total power of 120 W at 793 nm. The fiber laser resonator included two fiber Bragg gratings that helped to match the emission wavelength to the peak absorption band of Ho:YAG at 1908 nm. The laser output was coupled into a fiber with 400 µm core diameter.

The maximum demonstrated output power of the fiber laser was 48 W. However, due to its susceptibility to overheating when operating at high power, the output of the laser was kept below 13 W in order to mitigate the risk of failure. The available pump power was sufficient for the Ho:YAG laser and the fiber laser showed power stability of about 0.2%.

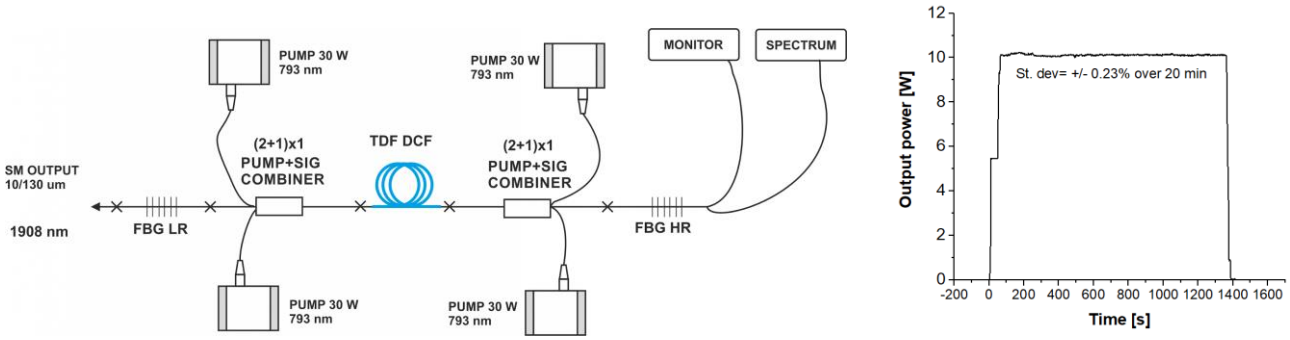

Figure 3 – Scheme of the 1.9-µm pump Tm:fiber laser (left) and its measured output power stability over 20 minutes

3.3. Holmium thin-disk laser development and testing

The output fiber of the pump laser was connected to the thin-disk gain module using a custom-made SMA-to-LLK-A adaptor. The imaging optics of the gain module were selected so the pump light was focused 32-times on an area with 1.6 mm diameter on the disk, achieving total absorption of the pump light.

Crytur s.r.o.
Na Lukách 2283
Turnov, 511 01
Czech Republic

26.1.2024

To obtain laser action, the disk in the gain module was placed in an optical resonator. A simple V-shaped cavity configuration with a 3-m concave mirror and flat output coupling mirror was selected to obtain robust and stable laser operation; the mirror positions were optimized for single-mode operation for the entire pump power range. Since Ho:YAG is an isotropic material, a Brewster plate (in our case from undoped YAG) in the cavity was necessary for generating a linearly polarized beam that could be later easily and arbitrarily attenuated.

Disks of both thicknesses were tested. While the thicker (400-µm) disks allowed to obtain somewhat higher output power (by about 15%) than the 250-µm disks thanks to higher gain, they also reached higher temperatures – up to 90 °C at 10-W pumping, while the thinner disks were only at 63 °C when measured using a thermal camera (see Fig. 2). Although the thicker disks were not at its damage limit, we chose the thinner disks for further development for their lower thermal deformation and better potential. This setup with the 250-µm disk and 5% output coupling mirror was used for performance tests in Phase II.

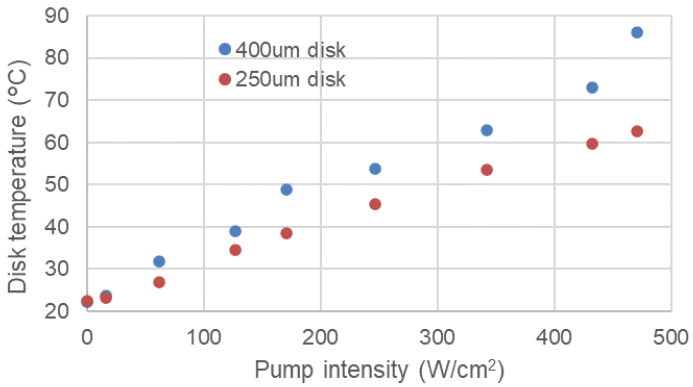

Figure 4 – Temperature of thin disks for various pumping levels

4. Characterization of the laser source parameters: the proof-of-concept

At the end of the Phase II of the project it was possible to perform the performance test of the main laser sources. Within the test it was demonstrated that it was possible to meet the proof of concept parameters that have been defined as ca. 5W output power with the Ho:YAG thin-disk solid-state free space laser working in the laboratory. The measured parameters are:

Maximum output power	6.2 W at 13 W pump
Power stability (RMS)	< 0.5 % over 1 hour at 5 W
Slope efficiency	54%
Central emission wavelength	2095 nm
Available wavelength tuning range	2014 – 2131 nm
Beam quality M^2	< 1.1 (1.0 at 2 W)
Output beam diameter ($1/e^2$)	15 mm

Crytur s.r.o.
Na Lukách 2283
Turnov, 511 01
Czech Republic

26.1.2024

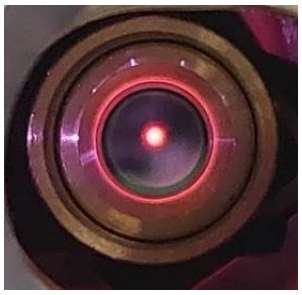

Figure 5 - Laser pump spot

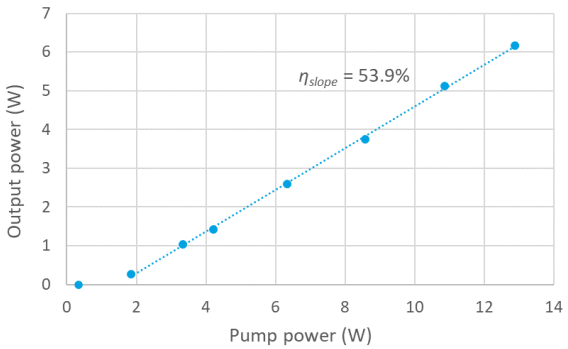

Figure 6 – Laser output vs. pump power

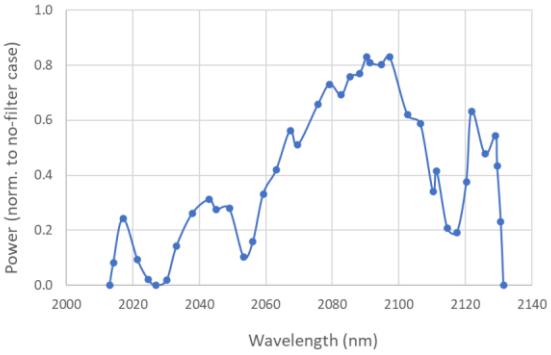

Figure 7 - Available wavelength tuning range with a birefringent plate in the cavity

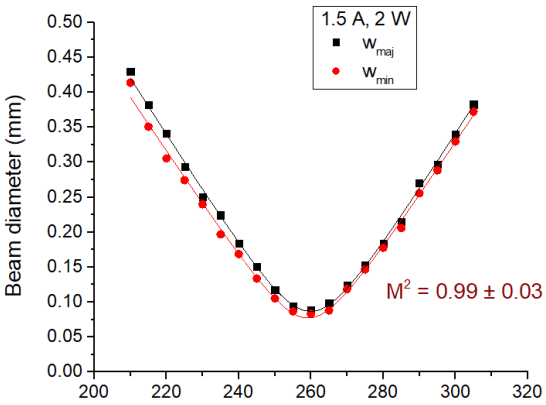

Figure 8 – Measured output beam quality

5. WP2: Laser transmitter and the laser receiver system

To be able to characterize the main laser beam parameters when propagated across short- and medium-range distances, the system of laser transmitter and laser receiver has been designed and prepared. Also a system of support laser beams with lasers at different wavelengths has been prepared.

5.1. WP2 - Laser source - transmitter design and preparation and final parameters

In the design phase, the main output laser beam parameters were defined as: 25 mm beam diameter, 50 µrad beam divergence, single-mode Gaussian profile, and 5W optical power. The last lens focal length is 200 mm (or 300 mm with alternative lens configuration). The beam calculated beam size after propagation through air: 25 mm at 20 m, 33 mm at 200 m, and 110 mm at 1 km.

The final design layout of the laser main source including all optical elements used in the setup for the laser transmitter was defined as shown in Figure 13. The setup includes the pump laser, the thin-disk module with the Ho:YAG thin-disk, and the optical resonator. The resonator is followed by the beam expander I and beam expander II setup. The attenuation of the beam is adjusted by a motorized beam attenuator. The final beam is steered and aligned with the set of 2-inch mirrors.

Crytur s.r.o.
Na Lukách 2283
Turnov, 511 01
Czech Republic

26.1.2024

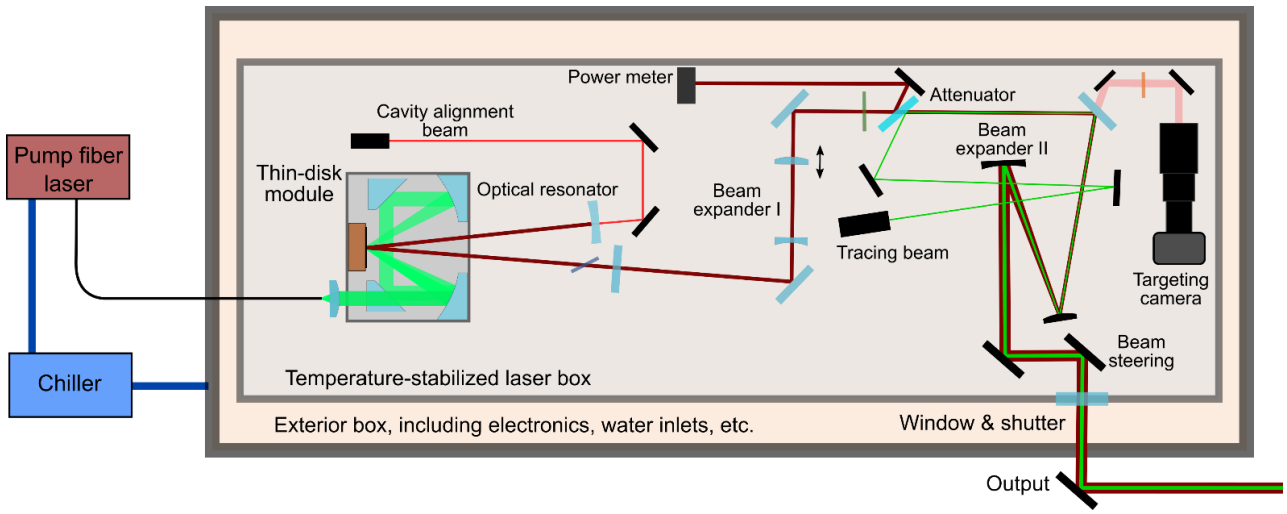

Figure 9 - Final design of the system of laser transmitter

During the development of the transmitter, it turned out that the clear aperture of the 2-inch optics, when used at an angle of incidence of around 45 degrees, is not large enough to transmit a 25-mm beam without diffraction (which became apparent after ca. 10 m propagation of the beam), which would make the beam unusable. To amend this, the beam expanders were modified to yield an output beam with only 15 mm diameter. This resulted in a somewhat more diverging output beam, with a minimum diameter after 500 m propagation of about 100 mm, which was still acceptable for the experiment in Phase III.

All optical and optomechanical components forming the main laser, laser transmitter, are integrated within the compact temperature-stabilized laser box. The laser box also encloses the sensitive components providing shielding against dust and humidity from the outer environment. The main laser box is integrated within the exterior box that houses electronics and connections for water, power, and remote control connections. The laser box including all components is in Figure 10.

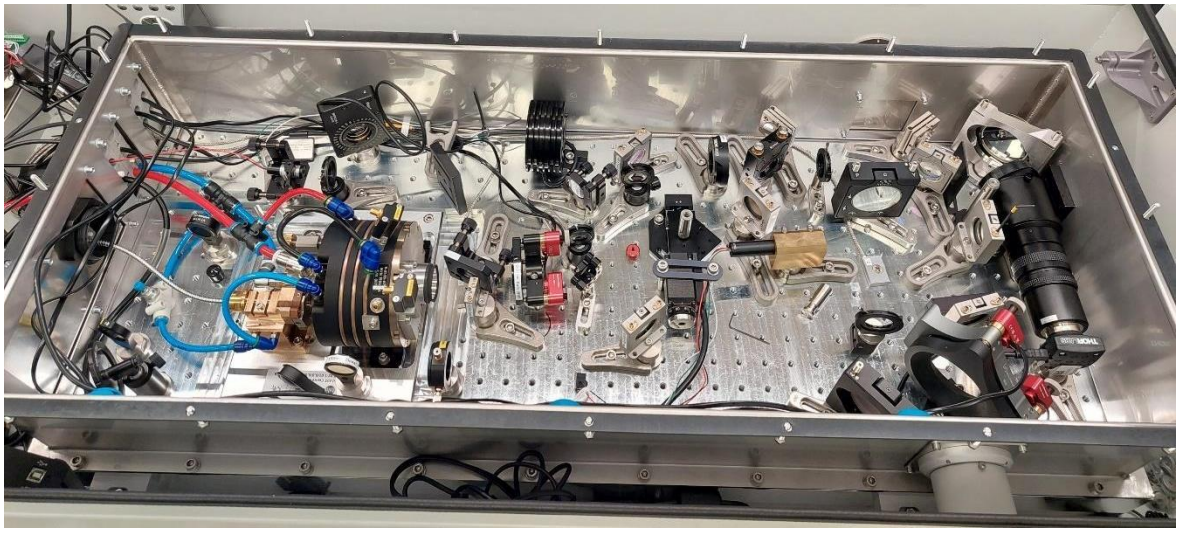

Figure 10 - Final layout of the laser transmitter

Crytur s.r.o.
Na Lukách 2283
Turnov, 511 01
Czech Republic

26.1.2024

The main laser box was designed to be portable using a trolley with wheels allowing it to transport all the necessary parts. The laser chiller is standalone and also portable. The portable trolley with the main laser 3D model is in Figure 11, Figure 12 shows the final laser on the portable frame in HiLASE laboratory. The dimensions of the main laser box including the weather-proof shielding are: 1300 x 550 x 270 mm.

Figure 11 - 3D model design of the portable laser transmitter box

Figure 12 - The main laser transmitter as prepared at HiLASE laboratory

The final beam parameters were measured in the beginning of the Experimental phase. The results are shown in section 6.

5.2. WP2 - Laser receiver cameras

The system of beam receiving cameras has been prepared to assess beam parameters after propagation in air. In the beginning, there were 2 concepts for monitoring the beam parameters: projection of the beam profile on the scattering screen and recording fluctuations of the parameters with cameras. The second option was observing partially reflected light from a sampler mirror with a set of two objectives and a focusing lens. Both scenarios are schematically shown in the pictures below:

Crytur s.r.o.
Na Lukách 2283
Turnov, 511 01
Czech Republic

26.1.2024

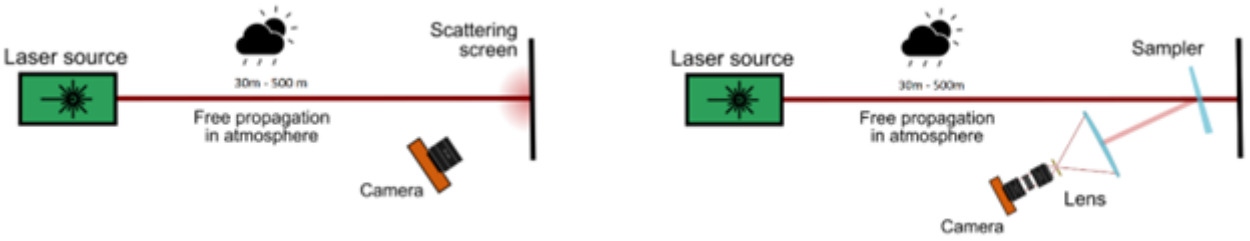

Figure 13 - Basic experimental layout for the atmospheric propagation tests

Following monitoring cameras were prepared for measurements with lasers:

NIT Tachyon camera with 128x128 px resolution, originally planned for measurement with the 2095 nm beam, which was, however, put as a backup option due to limited sensitivity and resolution.

Allied Vision Goldeye G-034 XSWIR 2.2 TEC2 InGaAs camera with sensitivity in the 1.4-2.2 µm region, 636 (H) × 508 (V) resolution, 15 µm × 15 µm pixel size and 210 fps; used for 2095, 1550 nm, and also 1064 nm beams (with lower sensitivity).

Figure 14 - the Allied Vision Goldeye G-034 XSWIR 2.2 TEC2 InGaAs camera

Allied Vision Manta G-125b silicon-based camera, max. 10 fps, with increased binning up to 8x8 pixels allowed to reach 116 fps; used for the measurement with 532, 640 a 1064 nm laser beams
Basler ace acA1920-150um Monochrome camera used for coarse alignment of the visible and 1064 nm beams.

5.3. Laser support systems - support laser beams

A set of support laser beams has been prepared to be able to compare propagation of the main laser with the wavelength of 2095 nm to the lasers at wavelengths used for laser free - space communication. The initial beam sizes of the additional laser beams were set to be close to the calculated beam size of the 2095 nm laser:

- **1550 nm,** 30 mW, short-wave infrared diode laser, initial beam size 14 mm
- **1064 nm,** 80 mW, short-wave infrared solid-state laser, fundamental transversal beam mode, initial beam size 15 mm

Crytur s.r.o.
Na Lukách 2283
Turnov, 511 01
Czech Republic

26.1.2024

- **640 nm,** 30 mW, red diode laser, beam profile not optimized, initial beam size 8 mm

- **532 nm,** around 1 mW at the output window of the 2100 nm laser box, solid-state laser, fundamental transversal beam mode, initial beam size 4 mm

The 640, 1064 and 1550 nm lasers use separate optics and optomechanics - optical mirrors and components with a 1-inch size having its mechanical base placed on the main 2095 nm laser box.
The 532 nm laser beam was prepared to be an alignment laser for the main laser. Therefore it was designed to use the same output optics and optomechanics as the 2095 nm laser, including the 2-inch exit mirror. The layout of the additional laser system is shown in Figure 15.

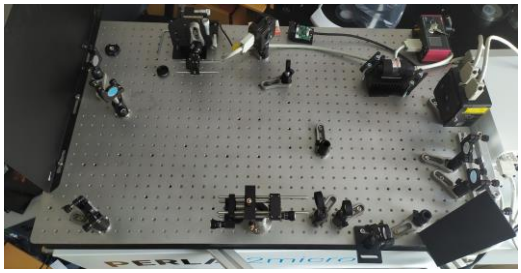

Figure 15 - Final layout of the system of additional lasers

6. WP 3: Experiment measurement

After a successful demonstration of the proof-of-concept parameters and performance of the 2095 nm laser in the HiLASE laboratory, the main laser with the support equipment has been moved from the Prague area to the Crytur premises in the city of Turnov located about 100 km away. Moving of the laser was a critical point due to the risk of damage caused by vibrations during the transport, extensive shocks, and possible contaminations. It is very likely that more sophisticated laser systems such as the 2095 nm laser get detuned and become dysfunctional.
However, this was not the case for the main laser and it was possible to continue with the measurement phase of laser beam propagation in Crytur, outside of the laser-dedicated laboratory.

6.1. Crytur building

The place for tests of the laser beam propagation was selected to be in the office-style laboratory in Crytur with windows to allow the beams to exit the laboratory and further in air propagation. The laboratory is located on the second floor. The Crytur building has not been constructed to provide high mechanical stability. The reason why this laboratory location was selected for the transmitter, was the access to power, access to the windows and clear

Crytur s.r.o.
Na Lukách 2283
Turnov, 511 01
Czech Republic

26.1.2024

Figure 16 - Laser transmitter in the Crytur laboratory

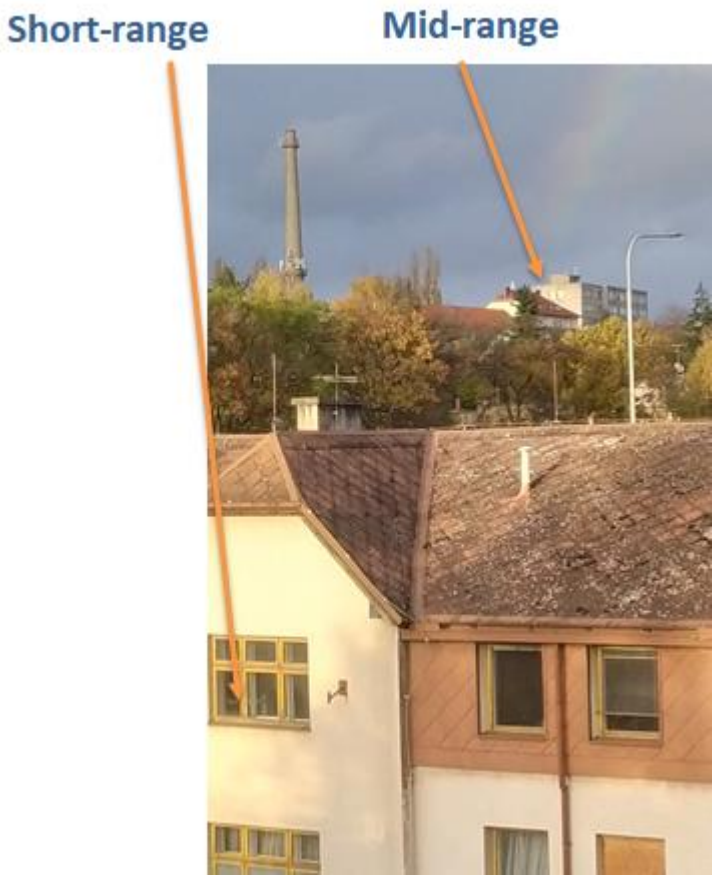

Figure 17 - View from the laser transmitter towards the receiver camera locations

visibility towards the short-range distance and mid-range distance targets. However, the mechanical stability of the lasers was directly dependent on the stability of the floor in the laboratory with the CNC machines and other heavy industrial machines running on the ground floor of the building.

6.2. Short-range distance measurements

The empty room in a separate building at a distance of 38m from the laser transmitter was chosen for the measurement over a short distance. Measurements of fluctuations of the main beam parameters were taken using the set of the Allied Vision Goldeye G-034 InGaAs camera and the Allied Vision Manta G-125b Si camera. Laser beams with wavelengths 2095 nm, 1550 nm, 1064 nm, 642 nm, and 532 nm were pointed at the plastic scattering screen. The setup of the measurement system with the standalone breadboard is in Figure 15. The following parameters were measured:

- Fluctuation of beam pointing: X and Y coordinates of the laser beam center
- Fluctuation of beam intensity: X and Y coordinates of the highest intensity pixels
- Integrated power of within the measurement frames
- Diameter of the beams: diameter across the minor and across the major elliptical axis

Crytur s.r.o.
Na Lukách 2283
Turnov, 511 01
Czech Republic

26.1.2024

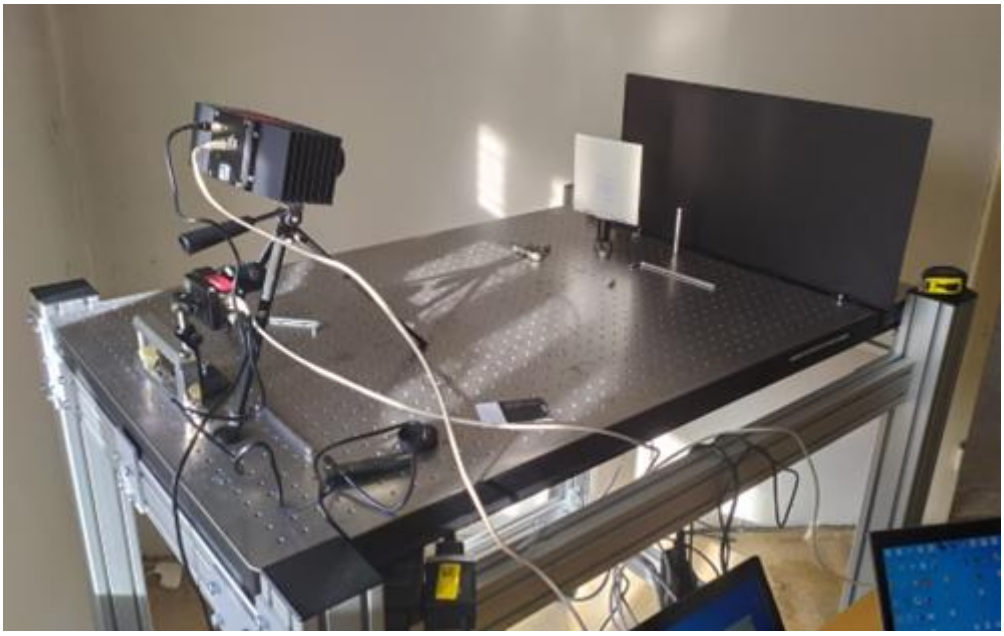

Figure 18 - System of laser receiver cameras for the short-range distance

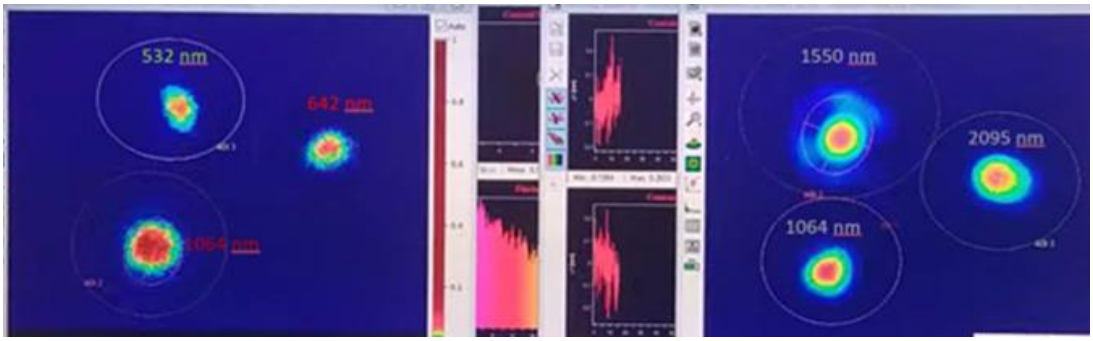

Figure 19 - Sample data from the measurement: Allied Vision Manta G-125b Si camera output on the left, Allied Vision Goldeye G-034 InGaAs camera on the right-hand side

The measurement of the laser beam parameters and their propagation over the short-range and the mid-range distance has been done using remote control of the cameras and the RayCi measurement software. The typical measurement interval was set to 2 minutes duration, camera setting as described in the 5.2 section. The sample screen from the measurement is in Figure 19.

6.3. Mid-range distance measurements

The measurements of fluctuations of the main beam parameters across the mid-range distance 521 m were recorded using the set of the Allied Vision Goldeye G-034 InGaAs camera and the Allied Vision Manta G-125b Si camera. Laser beams with wavelengths 2095 nm, 1550 nm, 1064 nm, 642 nm and 532 nm were pointed at the larger flat scattering screen.

Crytur s.r.o.
Na Lukách 2283
Turnov, 511 01
Czech Republic

26.1.2024

Figure 20 a - Mid-range distance (521 m) laser beams propagation measurements

Figure 20 b - Mid-range distance (521 m) laser beams propagation measurements under fog

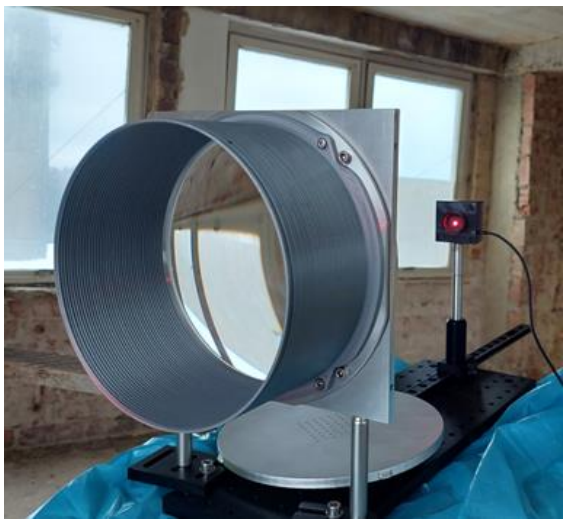

Figure 20 c - setup for measuring the power of large diameter laser beams; Figure 20 d - Receiver test: Photograph of the experimental team in short-wave infrared at the target area

Crytur s.r.o.
Na Lukách 2283
Turnov, 511 01
Czech Republic

26.1.2024

7. Results

The beam pointing fluctuation measurements were performed at various conditions:

- indoor measurement at 24°C temperature at a distance of 4 m, the goal was to confirm the mechanical stability of the laser sources,
- short-range measurement (over 38 m) in dry conditions, 0°C air temperature, wind from SW direction (beams were pointing roughly northwards) with speed of 2-3.5 m/s,
- mid-range measurement (over 520 m) in dry conditions, 0°C air temperature, wind from SW direction with speed of 1.5-3 m/s,
- mid-range measurement in moderate snowfall, -1°C air temperature, wind from N with speed around 1 m/s.
- mid-range measurement in light rain, 2°C air temperature, wind from NE with speed around 2 m/s,
- mid-range measurement in fog, 2°C air temperature, wind from NE with speed around 2 m/s.

During the indoor measurement, the beam position was recorded for all five laser sources over 25 seconds, with the cameras observing the beam spots from close distance (about 40 cm). The measured standard deviation of beam pointing (BP) from the central direction ranged from 4.7 µrad for the 1550 nm beam to 6.3 µrad of the 642 nm beam (as shown in Figure 21). For comparison, in the laser laboratory at HiLASE Centre with a monolithic concrete floor, the beam pointing fluctuation of the 2095 nm laser was determined as 2.0 µrad. The higher fluctuations at Crytur were caused primarily by the different construction of both buildings. Unfortunately, we had no means to evaluate the influence of the movement of the entire Crytur building, but we expect that it would contribute only to the low-frequency part of the BP fluctuation spectrum.

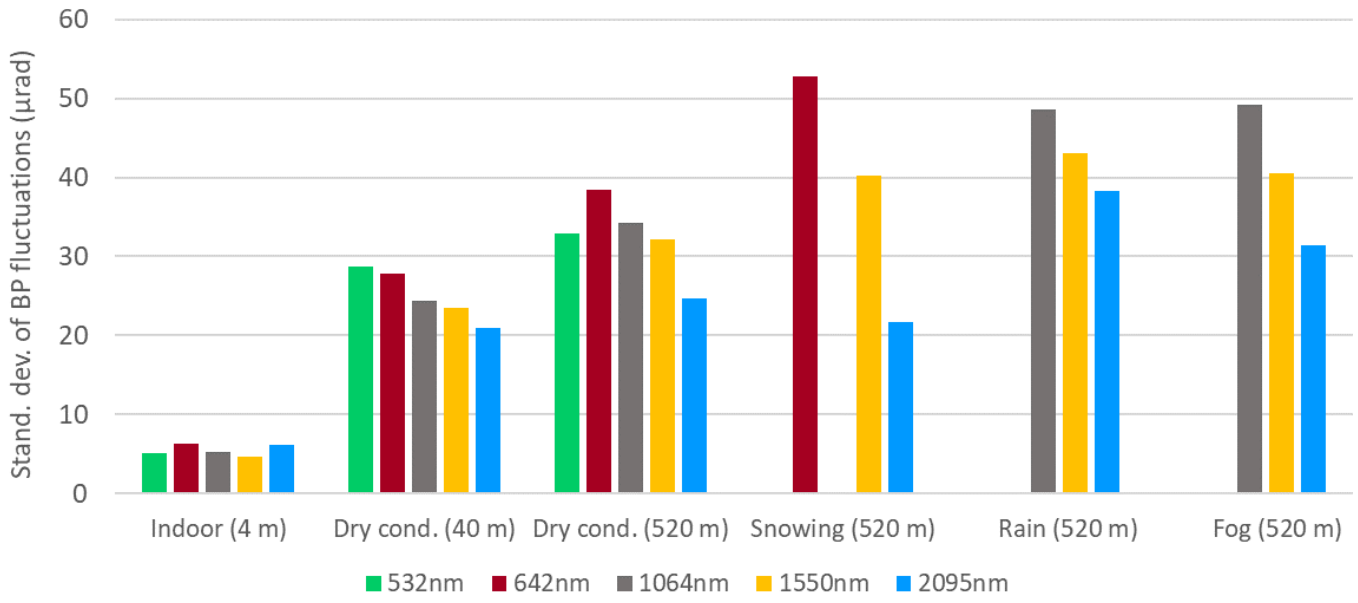

Figure 21 - Measured average beam pointing fluctuations for various wavelengths and conditions

At the short-distance atmosphere propagation test across 38 m at Crytur premises, it became apparent that the beam pointing stability decreased significantly. Over the distance of 38 meters, the laser beams were roughly 1-2 cm in diameter and traveled on the screen at a similar scale. At this distance, it was possible to record the position of all five beams simultaneously without significant issues. The 1064 nm beam was recorded using both cameras and their agreement served as a verification of the soundness of the two-camera setup. The BP fluctuations were

measured over 2 minutes six times and the results were averaged. The resulting BP fluctuations ranged from 20 to 30 µrad and were generally lower for longer wavelength beams.

Similar procedure was conducted for the mid-range measurement, pointing the laser beams over 520 m towards an abandoned factory. Aligning the beams precisely on the screen was more challenging, and with beam diameter increased due to diffraction (ranging from 8-cm 532 nm beam over 12-cm 2095 nm beam to 20-cm 1550 nm beam), their brightness dropped significantly, making them harder to detect. The substantial advantage of the 2095 nm and also 1550 nm wavelength was the low solar background in the short-wavelength infrared region - while it was difficult to steadily detect the 60-mW 1064 nm beam on a bright sunny day, power of only 5 mW was sufficient for viewing the 2095 nm beam with the SWIR camera. The 1-mW 532 nm beam could be measured only after sunset.

In dry conditions with moderate wind intensity, the beam pointing fluctuations increased by about 40% for the 1064 nm, 1550 nm, and 2100 nm at 520 m distance compared to the short-range measurement performed on the same day, while for the 2095 nm beam, it grew by 18% and only 15% for the 532 nm beam. This meant that still the fluctuations were generally more pronounced for shorter wavelengths, except the green beam, which was in this scenario on a similar level to the 1550 nm beam.

The measurements were carried out also in poor weather conditions, such as rain, snowfall or fog. Particularly the short-wavelength laser beams were oscillating noticeably more in weather with lower visibility, and the 2095 nm beam was the least affected one (as shown in Figure 21). Unfortunately, we could not measure strong wind, and during the snowfall, the 1064 nm beam was not available. The experimental data indicate that the advantage of the 2095 nm wavelength is more pronounced at worse atmospheric conditions.

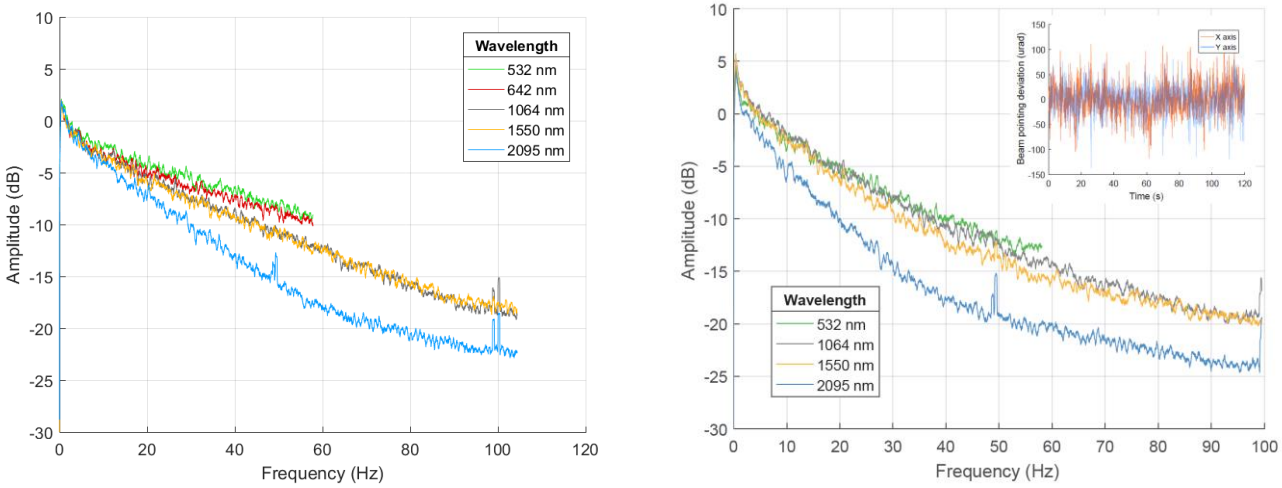

Figure 22 - Typical spectra of BP fluctuations (log scale) for short distance propagation in dry conditions (left) and long distance propagation in dry conditions (right) with a the temporal evolution of 2100 nm beam pointing (inset)

The beam pointing was primarily measured and statistically processed in the time domain, but additional insight could be gained also by studying the frequency spectrum of the fluctuations (obtained via FFT). The resolvable frequency was limited by the camera framerate (in some cases limited by long exposure time), and was around 105 Hz for the SWIR camera and 58 Hz for the silicon-based camera. The spectra (for good weather conditions shown in Figure 22) showed a typical hyperbolic decline of amplitude with frequency from the peak at 0 Hz. In poor weather, the fluctuation spectra seem to carry more information about the atmospheric conditions. Figure 23 compares fluctuation spectra for the 1550 nm and 2095 nm beam in various weather.

Crytur s.r.o.
Na Lukách 2283
Turnov, 511 01
Czech Republic

26.1.2024

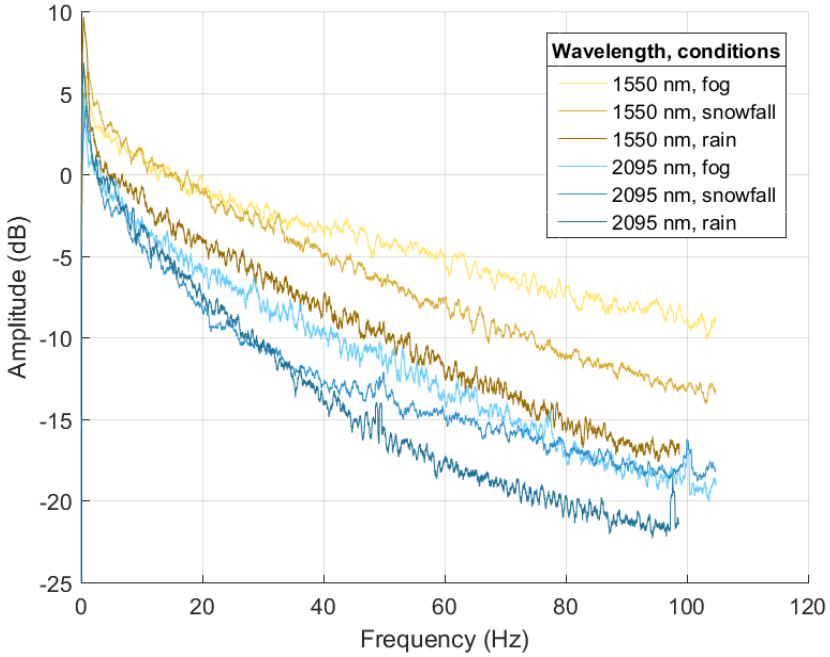

Figure 23 - Comparison of measured spectra at medium (520 m) distance for 1550 nm and 2095 nm laser beams in adverse weather conditions (light rain, moderate snowing, and fog)

Fluctuation peaks around 50 Hz and 100 Hz visible mostly in the spectra of the 2095 nm beam likely originate from the pump of water chiller (grid frequency) of the thin-disk laser and transferred through water channels to the 2095 nm laser and to some extent also mechanically to the other lasers.

For measuring atmospheric transmission, a setup using a power meter and an 8-inch lens with 400 mm focal distance was used (Figure 20c) for the beams with higher power (at 1064 nm fixed to approx. 80 mW and at 2100 nm several different power levels up to 0.5 W at 2095 nm, keeping it in Class 3R). First the measurement was conducted at short range at 40 meters in dry weather and later at 520 m in various conditions. In dry weather, the 480 m path difference resulted in transmission of approximately 88% for the 1064 nm beam and (96.0 ± 0.5)% for the 2095 nm beam (prediction from LOWTRAN model for summer atmosphere was 83% and 90%, respectively). In light fog, the measured transmission of the 1064 nm beam was 79%, while for the 2095 nm beam it was (92 ± 2)%. Finally, in light rain we measured transmission of the 2095 nm beam of (63 ± 5)%, meeting the prediction from LOWTRAN of 67% (1064 nm beam could not be measured in this case).

Crytur s.r.o.
Na Lukách 2283
Turnov, 511 01
Czech Republic

26.1.2024

8. Discussion

Numerical simulations of various configurations indicate one important fact: the longer the laser wavelength, which is not coinciding with the absorption band of an atmospheric component, the lower is its attenuation in comparison with the shorter wavelengths. Considering the recent availability of compact, reliable and high performance laser transmitter emitting at the wavelength of 2095 nm and the recent development of new optical detectors for this wavelength range, the laser operating at this wavelength is a logical candidate for optical communication and similar application in the Earth atmosphere.

The theoretical advantages of the 2095 nm wavelength are:

- lower beam propagation direction fluctuation due to the lower atmospheric refraction index,
- lower attenuation in propagation in the Earth atmosphere, namely under optically difficult conditions: rain, fog, dust, snowfall etc.,
- lower fluctuation in atmospheric propagation delay due to the lower atmospheric refraction index. This fact will result in higher limiting bandwidth in optical communication.
- lower background photon flux caused by Solar radiation and its scattering in the atmosphere. This fact might be crucial for quantum optical communication.

The measurement results of the beam propagation direction fluctuation shown in Figure 21 as well as the measured spectra presented in Figure 22 correspond with the above-mentioned expectation. One can conclude from the measurement results that the beam-pointing fluctuation is wavelength-dependent. The lowest pointing stability fluctuation has been measured for the 2095 nm laser beam.

From the results showing beam propagation under optically difficult conditions, it could be seen that fluctuation in beam propagation direction is the lowest for the 2095 nm beam. Also, the presented measurement results of the power attenuation using a power meter and 8-inch lens correspond with the expected lower attenuation of the 2095 nm wavelength.

The spectral range of atmospheric fluctuations is more or less overlapping with the spectrum of mechanical vibrations of buildings. That is why it was not possible to separate these two contributions directly. It is expected that mechanical vibrations of the building contribute only to the low-frequency part of the BP fluctuation spectrum, while the observed fluctuation spectra were broadband.

One of the possible further directions would be a measurement of time-of-flight fluctuations caused by atmosphere propagation is the most complex and difficult experiment that would characterize the 2095 mn wavelength from the point of ultra-short pulse propagation. Considering the values measured at the wavelength of 532 nm and the refraction index dependence on wavelength, the fluctuation of the order of 1 ps is expected. The measurement of this effect will need a laser transmitter generating pulses shorter than ca. 5 ps, a high sensitivity optical detector with ps time resolution, and ps timing device. A two-way propagation delay of the pulsed signal at 2095 nm wavelength over the ground distance of 5-10 km will be needed to be able to monitor the short-pulse beam delay fluctuations.

To employ the developed technology for optical communication, e.g. an earth-to-space communication link, the following tasks should be approached: modulating the CW output at a high rate to convey information, developing systems for automatic target tracking and beam steering, and reworking the transmitter in terms of robustness and compactness into an industrial-grade device. The output power could be straightforwardly scaled by a factor of 10 with only small changes in the current design.

Crytur s.r.o.
Na Lukách 2283
Turnov, 511 01
Czech Republic

26.1.2024

9. Conclusion

The new prototype of the thin-disk-based CW beam laser transmitter using Ho:YAG active material emitting laser at 2095 nm range has been developed for free-space optical communication. The 6-W single-mode high-power laser transmitter and the system of beam-receiving cameras for the range of wavelengths from 532 to 2095 nm have been constructed and tested in the laser-dedicated laboratory.

After the successful performance test of the laser sources, the newly developed TLR4 laser transmitter for the SWIR project has been moved outside the laser-dedicated-clean room laboratory to perform measurement experiments under real environment conditions. The laser transmitter has been used for a series of atmospheric propagation tests. The main CW laser output at 2095 nm in single mode has been directly compared to the additional laser sources. These lasers were CW operated at the wavelengths of 532, 640, 1064, and 1550 nm in single-mode beams. The optical spots of these lasers were monitored and analyzed after open-air propagation distances of 38 m and 521 m. Detailed experiment descriptions and individual results are in section 7. To summarize:

- Thanks to the measurement scheme all the completed measurements confirm the key fact that the beam propagation direction fluctuation (pointing stability) is lower at longer wavelengths. In all cases, these fluctuations were minimal at the new wavelength of 2095 nm.
- From the measurement results in Figure 21 it could be seen that the pointing stability is decreasing with increased beam propagation distance. The rate of decrease of the pointing stability was for the 2095 nm wavelength determined as the lowest one.
- Atmospheric attenuation – the results and limitations are analogical to the previous ones. One can conclude from the numerical computations performed in LOWTRAN in Phase I of the project that the optical signal attenuation at the 2095 nm wavelength is minimal under every atmospheric condition of the measurements for the considered spectral range. Our measured data confirm these calculations.
- Beam pointing stability is strongly influenced by mechanical vibrations of the laser setup and the building, where the lasers were installed. This factor has been limiting the possibility of measuring the beam propagation direction fluctuation directly and with high precision. It was possible to assess the fluctuation scale of the vibrations of the laser system and within the laboratory, but the task of measuring the movement of the building itself was beyond the scope of this project.

The atmospheric propagation of the laser in the SWIR project at the wavelength 2095 nm has been tested in a series of experiments. All these experiments proved the advantage of the novel wavelength 2095 nm from the point of view of atmospheric propagation in comparison to the shorter laser wavelengths. In addition, the validity of available optical models was demonstrated. The advantage of a longer wavelength of 2095 nm from a point of view of background photon flux has been described as well. The background photon flux at the new wavelength is about two times lower in comparison to the 1550 nm wavelength which might be crucial for quantum-based optical communication.